Modification of surface electronic properties on alloy surfaces: Standing waves on a Cu-9 at. % Al(111) surface observed by STM

Yinghui Yu, Keisuke Sagisaka,* and Daisuke Fujita
Advanced Nano Characterization Center, National Institute for Materials Science, 1-2-1 Sengen, Tsukuba, Ibaraki 305-0047, Japan
(Received 7 February 2009; revised manuscript received 18 May 2009; published 22 June 2009)

A direct and real-space study of the surface electronic structure on Cu-9 at. % Al(111) alloy surfaces was performed using low-temperature scanning tunneling microscopy. The standing waves on Cu-9 at. % Al(111)-(1×1) and $(\sqrt{3}\times\sqrt{3})R30°$ surfaces, which were obtained by controlling annealing temperature, were observed by differential-conductance mapping. Surface imperfection caused by segregation of aluminum atoms acted as static scattering centers in order to sustain the standing-wave formation. An analysis of the standing waves revealed a significant downward energy shift of the Shockley surface states on both surfaces. This shift is explained in terms of the strong redistribution of the surface electrons.

DOI: 10.1103/PhysRevB.79.235427 PACS number(s): 68.37.Ef, 61.66.Dk, 73.20.−r

I. INTRODUCTION

The so-called Shockley surface state with isotropic and parabolic energy dispersions on Cu(111), Ag(111), and Au(111) has been widely studied in the past years by angle-resolved photoemission electron spectroscopy (ARPES) and scanning tunneling microscopy (STM).[1–6] Among these studies, one of interesting aspects is the observation of standing waves (namely, an oscillation of local density of states in the Shockley surface state) by STM. The energy dispersion of the Shockley surface states is clarified by analyzing the standing-wave images, thereby, the effective mass m_e of the surface electrons [e.g., $0.39m_0$ for Cu(111),[1,2] where m_0 is the free-electron mass] is obtained by fitting the observed dispersion relation with a parabolic curve given by

$$E(k_{\parallel}) = E_F + E_0 + \hbar^2 k_{\parallel}^2/2m_e, \quad (1)$$

where E_F is the Fermi energy and E_0 is the surface-state band edge [e.g., −0.44 eV for Cu(111) (Ref. 2)].

In addition to the case of homogeneous metal surfaces, the modified Shockley surface states on binary metal alloys, such as Cu-Pd,[7] Cu-Al,[8,9] and Cu-Au,[10] were observed by ARPES. As for the copper-aluminum alloy system, while aluminum atoms are substituted randomly with copper atoms in the bulk, segregated aluminum atoms on the top layer can form an ordered $(\sqrt{3}\times\sqrt{3})R30°$ superstructure. The Shockley surface state on the (111) face of copper-aluminum alloy is located at the center of the surface Brillouin zone with the band-edge energy of about −0.8 eV for (1×1) and about −1.2 eV for $(\sqrt{3}\times\sqrt{3})R30°$.[8,9] This surface state is probably localized in the surface band gap (L gap) because alloying lowers the sp band levels of bulk copper by approximately 1 eV with respect to the Fermi level.[9] Therefore, the formation of surface standing waves in the Shockley state on the alloy is naturally anticipated. Moreover, in contrast to homogeneous surface potentials on metals,[2–6] random surface potentials induced by the aluminum atoms are expected to influence the standing-wave formation. However, to the best of our knowledge, relevant STM data on the copper-aluminum alloy have not yet been reported. Furthermore, while ARPES typically gives information about an electronic structure integrated over a large surface area (typically 10^2–10^3 μm), Fourier-transform (FT) STM yields both real- and reciprocal-space images related to the surface electronic structure of a very small (nanometer scale) and selected surface area.

In this current work, we used FT-STM to study the surface electronic structure of α-phase Cu-9 at. % Al(111) observe by differential conductance (dI/dV) mapping. We observed that the alloy surface has two types of structures [as already observed by low-energy electron diffraction (LEED)], i.e., (1×1) and $(\sqrt{3}\times\sqrt{3})R30°$ that possess different surface aluminum concentrations.[11–16] The obtained dI/dV images show that the standing waves are formed on both structures. The imperfections on the surfaces induced by aluminum atoms in copper acted as scattering centers that sustain the standing-wave formation. By analysis of the dI/dV images obtained at different bias voltages, we observed significant downward shifts of the Shockley surface state on both structures in strong contrast with that on pristine Cu(111). The observed electronic structures revealed parabolic energy dispersions of the surface electrons with isotropic effective masses and high electron densities.

II. EXPERIMENTS

The observations of the copper-aluminum alloy surface were carried out in a low-temperature STM system (Unisoku) with a base pressure of $<5.0\times10^{-9}$ Pa. The sample was a mechanically polished (111) face of α-phase copper-aluminum alloy containing 9 at. % randomly substitutional aluminum impurities in the bulk. The surface was cleaned by several cycles of argon sputtering and annealing. The annealing temperature was controlled at about 530 K to obtain the (1×1) surface and at about 850 K the $(\sqrt{3}\times\sqrt{3})R30°$ surface. The dI/dV images were recorded by a lock-in technique with a closed feedback loop. Sinusoidal-bias modulation voltage (peak to peak) was 10–20 mV at a frequency of 4.0–9.0 kHz. All STM images were acquired at about 79 K with electrochemically etched tungsten tips. In the power spectrum of the Fourier-transformed dI/dV images, lighter colors correspond to larger Fourier components.

III. RESULTS AND DISCUSSIONS

Figure 1(a) shows the topographic image of a pristine Cu(111) surface with a low defect density. A simultaneously

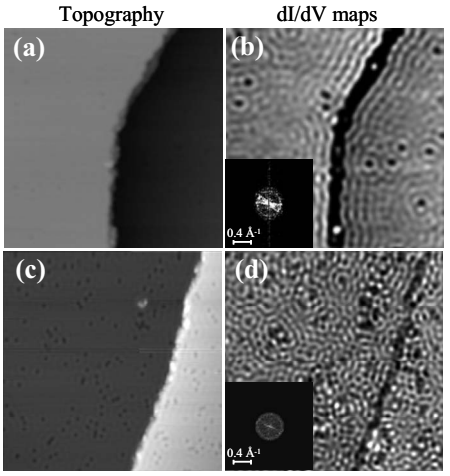

FIG. 1. Topographies and dI/dV maps on a Cu(111) surface at 79 K. (a) and (b) the surface with a low density of point defects (image size: 62×62 nm^2), (c) and (d) the surface with a high density of point defects (image size: 51×51 nm^2). $V_t=-0.20$ V and $I_t=1.0$ nA for all STM images. The insets in (b) and (d) show the Fourier-transform power spectra of the dI/dV maps.

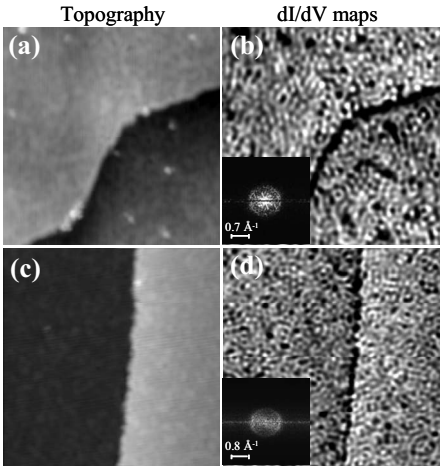

FIG. 2. Topographies and dI/dV maps on Cu-9 at. % Al(111) surfaces at 79 K. (a) and (b) (1×1) (image size: 30×30 nm^2), (c) and (d) $(\sqrt{3}\times\sqrt{3})R30°$ (image size: 25×25 nm^2). $I_t=1.0$ nA. $V_t=-0.20$ V for all STM images. The insets in (b) and (d) show the Fourier-transform power spectra of the dI/dV maps.

observed dI/dV image [Fig. 1(b)] detects standing waves that are induced by a step and several point defects. Each point defect causes concentric patterns of the standing waves around it while the step causes line-shaped patterns running parallel to it. These features are consistent with previous STM observations.[2] The topography in Fig. 1(c) shows another Cu(111) surface but with many point defects near a step, which were created by controlling the sputtering and annealing conditions. Auger-electron spectroscopy (AES) identified these defects as mainly carbon and oxygen. The feature of the standing-wave formation on the defective surface differs from that on the clean surface. The existence of many point defects not only makes the patterns of the standing waves intricate but also suppresses the formation of the line-shape patterns around the step, as observed in Fig. 1(d).

As already known from LEED and AES,[11–16] there are two types of surface structures, (1×1) and $(\sqrt{3}\times\sqrt{3})R30°$, on the Cu-Al(111) surface. Figure 2 shows topographic and dI/dV images observed on the Cu-9 at. % Al(111)-(1×1) [(a) and (b)] and $(\sqrt{3}\times\sqrt{3})R30°$ [(c) and (d)] surfaces. On both surfaces, the two terraces separated by a step look topographically inhomogeneous [Figs. 2(a) and 2(c)]. The spatial resolution of the images in Fig. 2 was limited because comparatively large sample bias (−0.2 V) and low tunneling current (1.0 nA) were used. However, the atomically resolved images in Ref. 17 reveal that this fluctuation on the surface arises from the short-range ordering of the excess aluminum atoms and dislocations in the top layer. Meanwhile, the dI/dV images in Figs. 2(b) and 2(d) show complicated patterns different from the topographic images in Figs. 2(a) and 2(c). The periodicity of the spatial distributions of the observed patterns increases with sample bias voltages. This bias-dependent feature is consistent with that of the standing waves on noble-metal surfaces.[2–6] Moreover, the previous ARPES observations revealed a Shockley surface state with nearly free electrons on copper-aluminum alloy surfaces.[8,9] We therefore conclude that the dI/dV maps in Figs. 2(b) and 2(d) reveal the standing waves formed in the Shockley state on the alloy.

The formation of the standing waves is sustained by electron-wave scatterers such as a defect and a step. As seen on the clean Cu(111) surface in Fig. 1(b), the existence of a step usually causes the line-shape patterns running parallel to the step while a point defect causes concentric patterns around it. In contrast, the surface with high defect density $(6.3\times10^{16}$ m$^{-2})$ in Fig. 1(d) displays a different feature, that is, superposition of concentric standing-wave patterns makes more complicated patterns across the surface. As a result, the line-shape patterns of standing waves near the step are hardly seen. Similarly, standing waves on the copper-aluminum surface are characterized as intricate circular shapes. On the alloy surface, the dominant scatterer is the fluctuation of the local aluminum density and dislocations as seen in Ref. 17. From our AES analysis,[13] we estimated the aluminum concentration in our sample surface to be approximately 16 at. % for the (1×1) surface and 36 at. % for the $(\sqrt{3}\times\sqrt{3})$ surface. These values can be converted to the average density of aluminum atoms, namely, 2.8×10^{18} m^{-2} for the (1×1) surface and 6.3×10^{18} m^{-2} for the $(\sqrt{3}\times\sqrt{3})$ surface. Since the valence electronic structure of aluminum $(3s^23p^1)$ is different from copper $(3d^{10}4s^1)$, it is conceivable that the local surface potential near aluminum atoms is modulated across the alloy surface. On our Cu-Al(111)-(1×1) surface, the aluminum concentration was 16 at. %; accordingly, the surface should include a small amount of local $(\sqrt{3}\times\sqrt{3})$ patches besides the (1×1) domains with randomly distributed aluminum atoms. Such surface features should act as static scattering centers for the standing waves in Fig. 2(b). Furthermore, even on the $(\sqrt{3}\times\sqrt{3})$ surface, there are many aluminum vacancies and dislocations caused by the improper aluminum stacking.[17] These defects, separated by several nanometers, create the standing waves on the $(\sqrt{3}\times\sqrt{3})$ surface [Fig. 2(d)]. In case of both alloy surfaces, similar to the case on the Cu(111) surface in Fig. 1(d), the existence of many

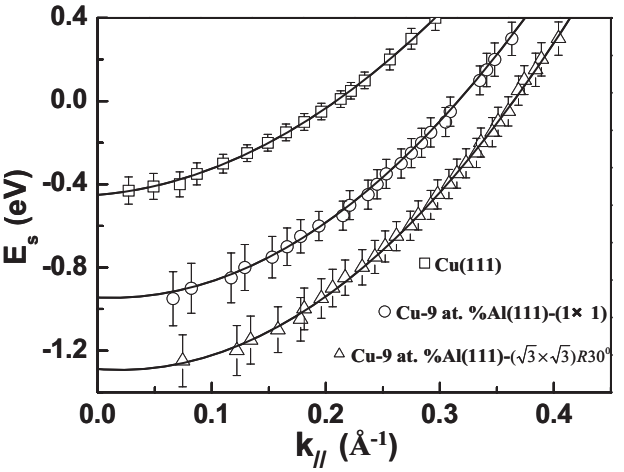

FIG. 3. Energy dispersion of the surface states on Cu(111), Cu-9 at. % Al(111)-(1×1), and $(\sqrt{3}\times\sqrt{3})R30°$ surfaces. The solid curves are fitted by using a parabolic function Eq. (1).

scattering centers screens the role of steps in creating the line-shaped standing waves near the step.

The insets in the dI/dV images of Figs. 1 and 2 are the corresponding FT images. A ring pattern is observed around the image center indicative of a free-electron-like surface state with isotropic effective mass[2–5] while the low-k features seen within the ring is derived from the step.[18] In a simple "hard-wall" model,[19,20] the wave number $k_{\|}$ of the surface states parallel to the surface at the applied bias voltage V_t [e.g., 0.28 $Å^{-1}$ for the (1×1) surface in Fig. 2(b)] can be obtained directly from half of the radius of the ring in the FT images originating from the standing waves. Plotting $k_{\|}$ obtained by the FT analysis of dI/dV images for different bias voltages provides the dispersion relation of the surface states on Cu(111) and Cu-9 at. % Al(111) as shown in Fig. 3. The dispersion relation is well fitted by a parabolic function of Eq. (1) with a fitting parameter m_e (the effective mass of the surface electrons). The bottom energy of the surface states, i.e., the surface-state band edge E_0, appears when $k_{\|}$ is zero. The fitting curves of the surface-state dispersion intersect the Fermi level E_F giving the Fermi wave number k_F. The obtained E_0, k_F, and m_e are listed in Table I. The dispersion relation for Cu(111) is consistent with the previous results observed by ARPES (Ref. 1) and STM.[2,5] On the other hand, the dispersion curves for Cu-9 at. % Al(111) are significantly shifted to lower energies compared to that of the pristine Cu(111). As seen in Table I, the band edges on Cu-9 at. % Al(111) are shifted by about 0.52 eV for (1×1) and by about 0.87 eV for $(\sqrt{3}\times\sqrt{3})$. Correspondingly, m_e and k_F on (1×1) ($0.39m_0$ and 0.31 $Å^{-1}$) and $(\sqrt{3}\times\sqrt{3})$ ($0.37m_0$ and 0.37 $Å^{-1}$) are different in comparison with those on Cu(111) ($0.40m_0$ and 0.21 $Å^{-1}$). Furthermore, the electron density at E_F $(k_F^2/2\pi)$ is calculated as 1.5×10^{18} and 2.2×10^{18} m^{-2} for (1×1) and $(\sqrt{3}\times\sqrt{3})$, respectively, in contrast to the value for Cu(111) (about 7.0×10^{17} m^{-2}). These results indicate that alloying strongly shifts downward the Shockley surface states on Cu-9 at. % Al(111). In addition, the observation of clear standing waves implies that the shifted Shockley surface state of the alloy is still situated in the surface band gap, which is consistent with the previous ARPES results that detected a downward shift of the sp bands of a bulk Cu-Al alloy by approximately 1 eV.[9]

The surface bond lengths of a bimetallic alloy are typically different from those of the parent metals giving rise to "strain effects" that modify the electronic structure of the metal through changes in orbital overlap. Moreover, the presence of aluminum atoms changes the electronic environment of neighboring copper atoms resulting in modifications of the electronic structure termed "ligand effects." It has been proved theoretically and experimentally that both effects generally change the energies of Tamm-type surface states (d electron related).[21–23] However, this effect on surface states is generally weak (<0.2 eV), in other words, it does not agree with our observation on the significant modification of the Shockley surface states (sp electron related).

The great modification of the Shockley surface state may be explained in terms of a strong redistribution of the surface electrons. Our AES investigation,[13] as well as others,[15] shows a feature referred as "splitting" of the Al LVV Auger lines with energies of about 64 and 68 eV on copper-aluminum alloy surface, indicating that sp bands of aluminum impurities hybridized with the d bands of copper.[24,25] As a result of the hybridization, strong redistributions of the sp surface electrons occur and form bonding and antibonding orbitals near the d band edges (about 2.0 eV below Fermi level).[26] The antibonding orbital filled with sp electrons shows a nearly free-electronlike feature and, thus, forms the Shockley surface states on Cu-9 at. % Al(111). Moreover, in the periodic table aluminum is located in a column with two more valence electrons than noble metals. By introducing the substitutional aluminum impurities in copper, the electrons of aluminum can transfer to neighboring copper atoms.[27] Consequently, the sp band (the Shockley surface state) should be significantly redistributed and lowered to accommodate the additional electrons from aluminum. Downward energy shifts and the higher electron densities are therefore observed on the Shockley surface states of Cu-9 at. % Al(111) compared with those of Cu(111). In

TABLE I. Surface-state b and edges E_0, Fermi wave number k_F, and the effective mass m_e of the surface electrons on Cu(111), Cu-9 at. % Al(111)(1×1), and $(\sqrt{3}\times\sqrt{3})R30°$ surfaces. The values in parentheses are quoted from Refs. 8 and 9.

Metal surfaces	E_0 (eV)	k_F ($Å^{-1}$)	$m_e(m_0)$
Cu-9 at. % Al(111)-(1×1)	−0.95(−0.80)	0.31 (0.29)	0.39 (0.40)
Cu-9 at. % Al(111)-$(\sqrt{3}\times\sqrt{3})R30°$	−1.30(−1.18)	0.37 (0.35)	0.37 (0.39)
Cu(111)	−0.43	0.21	0.40

fact, the amount of the surface-state shift depends on the concentration of aluminum. A greater amount of aluminum is segregated on the $(\sqrt{3}\times\sqrt{3})$ surface than on the (1×1) surface, consequently, a stronger redistribution of the surface electrons occurs on the $(\sqrt{3}\times\sqrt{3})$ surface. In turn, a greater energy shift of the surface states is observed on the $(\sqrt{3}\times\sqrt{3})$ surface to accommodate the greater amount of electrons from aluminum as suggested by a theoretical calculation.[28]

The current study on the surface-state dispersions of the Cu-9 at. % Al(111) surface resulted in larger downward shifts compared to the ARPES measurements performed by Asonen *et al.*[8,9] (see Table I). Our Cu-Al(111)-(1×1) surface was mildly annealed to about 530 K after sputtering. The concentration of aluminum atoms on the surface confirmed by AES was 16 at. %, which indicates that aluminum atoms were slightly segregated to the surface. On the other hand, Asonen *et al.*[8,9] prepared their surface by sputtering without annealing. The concentration of aluminum on their surface remained the same as in the bulk (10%). As discussed above, the higher concentration of aluminum atoms induces greater shift of surface states. This should be the reason for the inconsistency regarding the (1×1) surface between the present and previous studies. If we apply the same discussion to the disagreement of band shift on the $(\sqrt{3}\times\sqrt{3})$ surface, we see that our $(\sqrt{3}\times\sqrt{3})$ surface contains more aluminum atoms than that in the previous study. We confirmed the saturation of aluminum segregation on our $(\sqrt{3}\times\sqrt{3})$ surface using AES before STM observations but the concentration of aluminum on the $(\sqrt{3}\times\sqrt{3})$ surface used in the ARPES experiment is not known. Furthermore, the ARPES measurement on the $(\sqrt{3}\times\sqrt{3})$ surface showed broad spectra, possibly due to the limited device resolution and the measurement performed at room temperature. These limitations may have influenced their analysis to determine the surface-state dispersion.

IV. SUMMARY

Low-temperature STM was applied to observe the standing waves on the Cu(111), Cu-9 at. % Al(111)-(1×1), and $(\sqrt{3}\times\sqrt{3})R30°$ surfaces. The standing-wave patterns on the alloy surfaces were more complicated than those on the Cu(111) surface because of the existence of a number of scattering centers. The energy dispersion of the Shockley surface states was also examined through Fourier analysis of the dI/dV maps. It was observed that significant shifts of the energy levels occurring on the alloy surface coincide with the modification of the effective mass of surface electrons, the Fermi wave number, and the surface electron density. Such a modification of the surface electronic properties on the alloy surfaces is attributed to the strong redistribution of the surface electrons.

ACKNOWLEDGMENTS

This work was partly supported by World Premier International Research Center Initiative (WPI Initiative) on Materials Nanoarchitectonics and by KAKENHI (Grant No. 19740185), MEXT, Japan.

*Author to whom correspondence should be addressed; sagisaka.keisuke@nims.go.jp

[1] P. O. Gartland and B. J. Slagsvold, Phys. Rev. B **12**, 4047 (1975).
[2] M. F. Crommie, C. P. Lutz, and D. M. Eigler, Nature (London) **363**, 524 (1993).
[3] Ph. Avouris, I. W. Lyo, R. E. Walkup, and Y. Hasegawa, J. Vac. Sci. Technol. B **12**, 1447 (1994).
[4] D. Fujita, K. Amemiya, T. Yakabe, H. Nejoh, T. Sato, and M. Iwatsuki, Phys. Rev. Lett. **78**, 3904 (1997).
[5] L. Petersen, P. T. Sprunger, Ph. Hofmann, E. Lægsgaard, B. G. Briner, M. Doering, H.-P. Rust, A. M. Bradshaw, F. Besenbacher, and E. W. Plummer, Phys. Rev. B **57**, R6858 (1998).
[6] T. Suzuki, Y. Hasegawa, Z.-Q. Li, K. Ohno, Y. Kawazoe, and T. Sakurai, Phys. Rev. B **64**, 081403(R) (2001).
[7] R. S. Rao, A. Bansil, H. Asonen, and M. Pessa, Phys. Rev. B **29**, 1713 (1984).
[8] H. Asonen and M. Pessa, Phys. Rev. Lett. **46**, 1696 (1981).
[9] H. Asonen, M. Lindroos, M. Pessa, R. Prasad, R.-S. Rao, and A. Bansil, Phys. Rev. B **25**, 7075 (1982).
[10] R. Courths, M. Lau, T. Scheunemann, H. Gollisch, and R. Feder, Phys. Rev. B **63**, 195110 (2001).
[11] R. J. Baird and W. Eberhardt, J. Vac. Sci. Technol. **18**, 538 (1981).
[12] M. Yoshitake, S. Bera, Y. Yamauchi, and W. Song, J. Vac. Sci. Technol. A **21**, 1290 (2003).
[13] Y. H. Yu, K. Sagisaka, and D. Fujita, Surf. Sci. **603**, 723 (2009).
[14] J. Ferrante, Acta Metall. **19**, 743 (1971).
[15] R. J. Baird and T. J. Potter, J. Vac. Sci. Technol. A **3**, 1371 (1985).
[16] R. J. Baird, D. F. Ogletree, M. A. van Hove, and G. A. Somorjai, Surf. Sci. **165**, 345 (1986).
[17] E. Napetschnig, M. Schmid, and P. Varga, Surf. Sci. **602**, 1750 (2008).
[18] This was confirmed by filtering out the low-k components within the ring from dI/dV images.
[19] L. Bürgi, O. Jeandupeux, A. Hirstein, H. Brune, and K. Kern, Phys. Rev. Lett. **81**, 5370 (1998).
[20] S. Pons, P. Mallet, and J. Y. Veuillen, Phys. Rev. B **64**, 193408 (2001).
[21] J. R. Kitchin, J. K. Norskov, M. A. Barteau, and J. G. Chen, Phys. Rev. Lett. **93**, 156801 (2004).
[22] J. R. Kitchin, J. K. Norskov, M. A. Brteau, and J. G. Chen, J. Chem. Phys. **120**, 10240 (2004).
[23] D. Sekiba, K. Nakatsuji, Y. Yoshimoto, and F. Komori, Phys. Rev. Lett. **94**, 016808 (2005).
[24] K. Tanaka, M. Matsumoto, S. Maruno, and A. Hiraki, Appl. Phys. Lett. **27**, 529 (1975).
[25] A. Hiraki, S. Kim, W. Kammura, and M. Iwami, Appl. Phys. Lett. **34**, 194 (1979).
[26] K. Terakura, J. Phys. Soc. Jpn. **40**, 450 (1976).
[27] T. Kravchuk, Yu. Bandourine, A. Hoffman, and V. A. Esaulov, Surf. Sci. **600**, L265 (2006).
[28] D. W. Bullett, Solid State Commun. **43**, 490 (1982).